ChemComm

COMMUNICATION

View Article Online
View Journal | View Issue

Cite this: *Chem. Commun.*, 2025, **61**, 8516

Received 18th March 2025,
Accepted 29th April 2025

DOI: 10.1039/d5cc01447f

rsc.li/chemcomm

Properties of $NaPF_6$ electrolytes and effect of electrolyte concentration on performance in sodium-ion batteries†

Darren M. C. Ould,[ab] Stefan Oswald,[ab] Holly E. Smith,[a] Christopher A. O'Keefe,[a] Tengfei Song,[bc] Emma Kendrick,[bc] Dominic S. Wright[ab] and Clare P. Grey*[ab]

Sodium-ion batteries offer improved sustainability over lithium-ion batteries, the benchmark electrolyte being 1 M $NaPF_6$ in carbonate-based solvents. This work investigates the properties of different electrolyte concentrations, finding that 1 M $NaPF_6$ offers the highest bulk conductivity. However, lower concentrations give comparable cycling performance in sodium-ion coin cells.

The global drive towards net zero carbon emissions requires suitable energy storage solutions. Currently, lithium-ion batteries (LIBs) are the leading rechargeable battery technology.[1,2] However, LIBs use resource critical materials, such as lithium and cobalt, which causes concerns regarding their long-term sustainability.[3–5] Sodium-ion batteries (SIBs) are a promising post-LIB technology that offer key sustainability advantages.[6,7] In addition to the greater abundance and more even global distribution of sodium deposits, SIBs allow for cobalt-free cathodes to be used, such as $NaNi_{0.33}Fe_{0.33}Mn_{0.33}O_2$ (NFM111). For the anode, SIBs commonly use hard carbon instead of graphite, which may be derived from bio-waste.[8,9] Moreover, the sustainability is improved by employing aluminium current collectors at the anode, in contrast to copper in LIBs.[10]

Although often overlooked, the electrolyte plays a crucial role in the battery as it is largely responsible for the practical accessible capacity, overall lifetime and safety.[11–13] The two most common electrolyte salt choices for SIBs are sodium perchlorate ($NaClO_4$) and sodium hexafluorophosphate ($NaPF_6$).[11,14] While the former is a popular choice for academic studies, the perchlorate anion is a strong oxidant and is unsuitable for commercial use. Moreover, recent work has shown $NaPF_6$-based electrolytes to be superior at high rate compared to using $NaClO_4$. This was partly explained by the decomposition of the PF_6^- anion to form an inorganic-rich cathode–electrolyte interphase (CEI), thus ensuring interface stability and inhibiting continual solvent decomposition and thus increased cell impedance.[15]

The use of $NaPF_6$ salt for the electrolyte formulation is attractive as $LiPF_6$ is commonly used in LIBs, which may accelerate electrolyte development.[16] The $NaPF_6$ salt has a relatively high decomposition temperature (starting at approximately 325 °C),[17] and when dissolved in carbonate-based solvents offers good ionic conductivity.[11] Moreover, studies on the passivation of aluminium current collectors have revealed that a passivating $AlF_3/AlO_{x/2}F_{3-x}$ film forms when using $NaPF_6$, helping to prevent aluminium corrosion. This forms due to the reaction of HF (produced from hydrolysis of $NaPF_6$) with Al_2O_3.[18,19] However, a drawback of $NaPF_6$ is its poor tolerance to moisture, producing NaF, PF_4O^-, POF_3 and HF *etc.* as hydrolysis products. HF and accompanying degradation products are found in electrolyte solutions that contain <20 ppm water.[20]

The effect of $NaPF_6$ concentration in the electrolyte has previously been studied in order to understand changes in the thermal stability,[21,22] ionic conductivity,[19,21–25] viscosity,[21–23] and transport properties.[25] However, the results vary depending on solvent choice and the concentrations studied. It has previously been shown from differential scanning calorimetry measurements that increasing the $NaPF_6$ concentration in ethylene carbonate: dimethyl carbonate (EC : DMC 1 : 1 wt%) from 0.3 M to 1.4 M lowers the crystallisation temperature (T_c), the temperature that in practice sets the absolute lowest working and storage limit.[22]

Multiple studies have investigated the ionic conductivity and the maximum values reported depend on the concentration range studied and solvents used. For example, when using $NaPF_6$ electrolyte in EC : DMC (3 : 7 wt%) between 0.4 M and 1 M, the 0.6 M solution gave the highest conductivity (6.8 mS cm^{-1}).[19] On the other hand, a separate study found a maximum ionic conductivity of 11.2 mS cm^{-1} at 1.2 M concentration in EC : DMC (1 : 1 wt%).[22] Moreover, studies on the transference number for

[a] *Yusuf Hamied Department of Chemistry, University of Cambridge, Lensfield Road, Cambridge, CB2 1EW, UK. E-mail: cpg27@cam.ac.uk*
[b] *The Faraday Institution, Quad One, Harwell Science and Innovation Campus, Didcot, OX11 ORA, UK*
[c] *School of Metallurgy and Materials, University of Birmingham, Birmingham B15 2TT, UK*

† Electronic supplementary information (ESI) available: Experimental details and electrochemistry procedures, NMR spectra. See DOI: https://doi.org/10.1039/d5cc01447f

$NaPF_6$ in ethylene carbonate: diethyl carbonate (EC : DEC 1 : 1 v/v) show the cation transference numbers decrease from approximately 0.5 to 0.3 when increasing the concentration from 0.1 M to 2 M $NaPF_6$.[25]

While fundamental properties of different $NaPF_6$ electrolyte concentrations have been investigated, few studies relate this to the impact on sodium-ion cycling. Instead, it is common to use a 1 M concentration, likely appropriated from LIBs. Previously, it has been shown that when using half-cells employing a $Na_xNi_{0.22}Co_{0.11}Mn_{0.66}O_2$ cathode, cells containing 1 M $NaPF_6$ in propylene carbonate electrolyte outperformed 0.1 M and 3 M electrolyte concentrations with respect to capacity and rate performance.[21]

This work investigates the effect on ionic conductivity, viscosity and diffusion of varying $NaPF_6$ electrolyte concentrations in an EC : DEC (1 : 1 v/v) solvent mixture. Extended galvanostatic cycling has been performed to evaluate their performance in SIBs.

To begin, pure $NaPF_6$ salt was synthesised following our previously reported procedure.[24] Electrolyte solutions were then prepared by dissolving $NaPF_6$ in a binary EC : DEC (1 : 1 v/v) solvent mixture. The $NaPF_6$ concentrations investigated were 0.25 M, 0.5 M, 1 M, 1.5 M and 2 M, which gave a broad range of low to high concentrations. Multinuclear NMR spectroscopy was used to check the purity and ensure that HF or other impurities were not present (Fig. S15–S22, ESI†).

To first assess the differences in the $NaPF_6$ electrolyte solutions, bulk conductivity measurements at 25 °C were recorded (Fig. 1 and Fig. S1, ESI†). The conductivity was initially found to increase with increased concentration, with the 1 M $NaPF_6$ solution giving the highest bulk conductivity (8.8 mS cm^{-1}, Fig. 1). However, increasing the concentration beyond 1 M gave a decrease in conductivity, despite having more charge carriers. The highest electrolyte concentration studied, 2 M, has a bulk conductivity similar to the 0.5 M $NaPF_6$ electrolyte, 7.2 and 7.4 mS cm^{-1}, respectively.

To explain the trend in the conductivity values, the dynamic viscosity of the different electrolytes, ionicity (Fig. S4, ESI†) and self-diffusion coefficients (D) of the PF_6^- anion and solvent molecules were determined. The viscosity is a crucial property of the electrolyte as highly viscous solutions will hinder the movement of ions and lower the conductivity. Moreover, the viscosity can impact wetting of the electrodes and separator.

The viscosity of the $NaPF_6$ electrolyte solutions expectantly increases across the series from 0.25 M to 2 M concentration, as more ionic interactions occur with increasing concentration (right-hand side of Fig. 1). The similarity of the conductivity values for the 1 M and 1.5 M $NaPF_6$ electrolytes, 8.8 mS cm^{-1} and 8.5 mS cm^{-1}, respectively, can therefore be seen as a trade-off between an increase in the number of conductive charge carriers present in solution *versus* the corresponding increase in the solution viscosity. This argument also applies to the similar conductivity values observed for the 0.5 M and 2 M electrolyte solutions.

To support the conductivity and viscosity measurements, the transport properties of the PF_6^- anion and solvent molecules were investigated by obtaining their self-diffusion coefficient (D) values (Fig. 2, Fig. S2 and Tables S1, S2, ESI†). This was performed by using ^{19}F and ^{1}H NMR diffusion-ordered spectroscopy (DOSY), respectively. The Stokes–Einstein equation states that for spherical, non-interacting particles, D should be inversely proportional to viscosity. In addition, other factors may affect D with changing concentration, including changes to the solvation shells of ions and ion–ion interactions. Using ^{19}F NMR DOSY, the D_{anion} of the PF_6^- anion decreases with increasing concentration. This is again explained by the increase in solution viscosity, as well as a likely greater degree of ion pairing (and potential aggregate formation) with increasing concentration.

Using ^{1}H NMR DOSY, the $D_{solvent}$ values for the EC solvent molecules follow the same trend as the PF_6^- anion. This can be explained by the increasing solution viscosity and a greater proportion of solvent molecules being incorporated into ion solvation shells at higher salt concentrations. At all concentrations, $D_{solvent}$ values for EC are higher than for the PF_6^- anion.

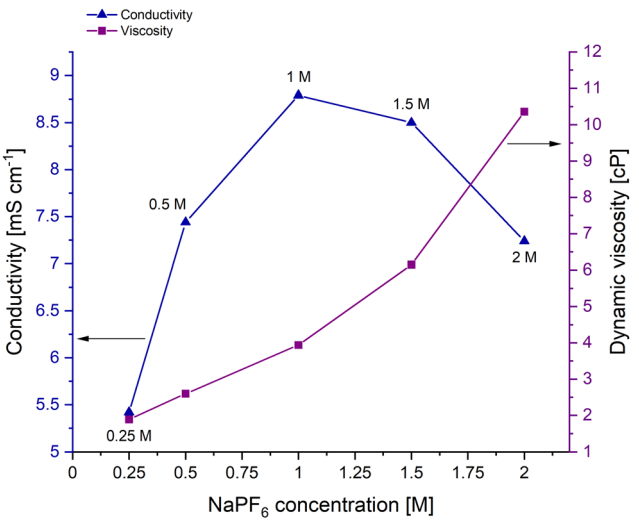

Fig. 1 Bulk conductivity (blue) and dynamic viscosity values (purple) of 0.25 M, 0.5 M, 1 M, 1.5 M and 2 M $NaPF_6$ in EC : DEC (1 : 1 v/v) electrolytes at approximately 25 °C.

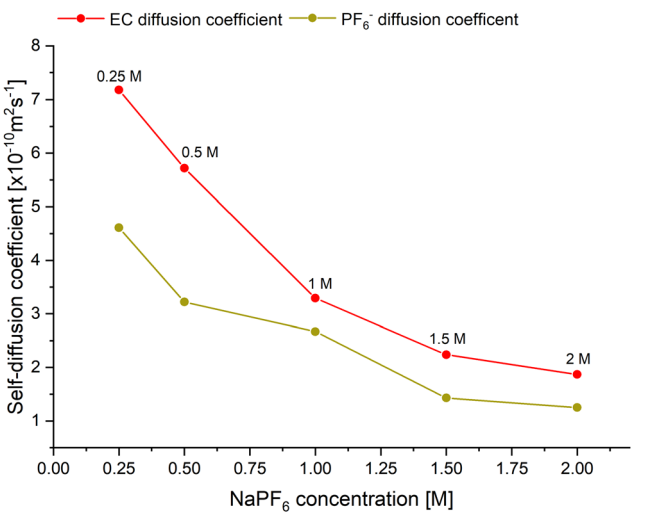

Fig. 2 Self-diffusion coefficients of the EC solvent molecule (red, ^{1}H DOSY NMR) and the PF_6^- anion (yellow, ^{19}F DOSY NMR) of 0.25–2 M $NaPF_6$ in EC : DEC (1 : 1 v/v) electrolytes.

Neutral solvent molecules are expected to experience less resistance moving through the solution than charged ions, particularly those that are not coordinated to Na^+, hence their higher D values.

Na^+ favours a five- or six-coordination geometry (*cf.* four-coordinate Li^+) and cyclic carbonates preferentially coordinate to Na^+ over linear carbonates. Thus, in the coordination shell of Na^+ the ratio of EC to DEC is greater than 1 : 1.[22] If we assume that four EC solvent molecules are coordinated to Na^+ at all electrolyte concentrations (see ESI† for further discussion), the percentage of free EC solvent molecules (not coordinated to Na^+) decreases from 87% in the 0.25 M $NaPF_6$ electrolyte to 47% in the 1 M $NaPF_6$ sample. For the 2 M $NaPF_6$ electrolyte, all the EC molecules would be coordinated to Na^+. $D_{solvent}$ values for EC and DEC solvent molecules were found to be similar across the concentration range measured (Table S1 and Fig. S2, ESI†).

Extended charge/discharge cycling was undertaken to understand whether the observed differences in conductivity, viscosity and ion transport would impact battery performance. For this, the electrolyte solutions 0.25 M, 0.5 M, 1 M and 2 M $NaPF_6$ in EC : DEC (1 : 1 v/v) were used. Coin cells were constructed using an NFM111 cathode and a hard carbon anode; glass fibre separator was used with 100 µl of electrolyte.

Before constructing full-cells (see ESI† for details), NFM111 and hard carbon were first assembled in half-cells against sodium metal, using 1 M $NaPF_6$ electrolyte. This was to understand the characteristics of the electrode materials and their voltage profile (Fig. S5 and S6, ESI†). These experiments revealed that the full-cells require cutoff voltages of 1.5 V and 4.0 V, offering an expected capacity of 138 mA h g^{-1}. In addition, scanning electron microscopy (SEM) images of the pristine cathode and anode were obtained (Fig. S11–S14, ESI†).

The cycling protocol for the NFM111 *vs.* hard carbon cells (capacity ratio of anode to cathode is 1.2 : 1) involved two C/20 formation cycles with a cutoff voltage of 4.0 V, followed by two 2C and 46 C/2 cycles. This set of 50 cycles was then repeated six times, giving a total of 300 cycles. The three different C-rates employed in the cycling procedure help assess different degradation mechanisms, discriminating loss of sodium inventory or active material from kinetic limitations in the different concentration electrolyte solutions.

All four $NaPF_6$ electrolytes underwent cycling, where little/no significant differences were observed with respect to initial and final capacities (Fig. 3). The C/20 rate cycles gave the highest initial capacity, followed by C/2 and then 2C rates, giving the expected decrease in capacity with higher discharging rates. The approximate initial capacities were 115, 105, and 95 mA h g^{-1} for the cycles at C/20, C/2, and 2C, respectively. Interestingly, although the discharge capacity decreases with increasing cycle number for all three C-rates, the greatest capacity drop is observed for the 2C rate. For example, by comparing the first and last 2C cycle for 1 M $NaPF_6$ electrolyte, the capacity retention was 61%. The same analysis for the C/20 cycles gave a capacity retention of 86% and for the C/2 cycles it was 66%. It is hypothesised this is a kinetic effect caused by greater resistance on the anode and/or cathode.

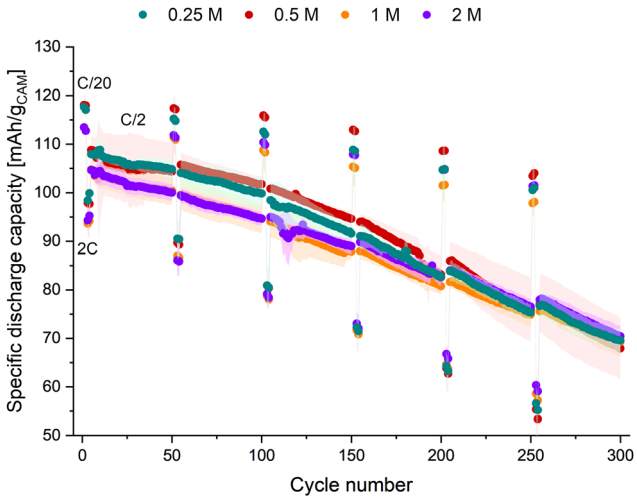

Fig. 3 Specific discharge capacity *vs.* cycle number using NFM111 cathode and hard-carbon anode. The applied C-rates of C/20, 2C, and C/2 were calculated based on the expected capacity of 138 mA h g^{-1} of the cathode, using cell voltage limits of 1.5 and 4.0 V. Electrolyte is 0.25 M (green), 0.5 M (red), 1 M (orange) and 2 M (purple) $NaPF_6$ in EC:DEC (1 : 1 v/v). Error bars display standard deviation of 2–4 coin cells, cycled at 21 °C.

Thus, these cycling results reveal that under these testing conditions, the lower concentration electrolyte solutions perform as well as the conventional 1 M electrolyte concentration. Despite the approximate 50% lower bulk conductivity of the 0.25 M electrolyte compared to the 1 M electrolyte, the discharge capacities are not affected, even at the moderately high rates of 2C. For the 2 M $NaPF_6$ in EC:DEC electrolyte, although there are reports of improved interphase stability with increasing electrolyte concentration, no benefits in cycling were observed.[26] This may be due to reduced ion mobility. As there was no significant change in cycling performance with different electrolyte concentrations, it is hypothesised that these cells are limited by either the charge-transfer resistance or solid-state diffusion of Na^+ in the active electrode materials, rather than electrolyte concentration.

In addition, cycling was performed at 50 °C and compared to the results at 20 °C, assessing the effect of elevated temperature on battery performance (Fig. 4). An electrolyte that can perform well at elevated temperatures is advantageous as it potentially negates the need for expensive cooling systems. For this, additional coin cells were constructed using NFM111 and hard carbon electrodes. These cells were formed using two C/20 cycles at room temperature, after which they were cycled at a rate of C/2 for both charge and discharge at either 20 °C or 50 °C.

For all electrolyte concentrations, the initial capacity was approximately 15 mA h g^{-1} higher for the cells cycled at 50 °C compared to 20 °C. However, the capacity retention was poorer for the high-temperature cells (Fig. 4 and Fig. S7, S9, ESI†). For example, after 250 cycles, the capacity retention for the 1 M cells at 50 °C was 78%, while the 1 M cells at 20 °C had a higher capacity retention of 87%. The higher initial capacity of the 50 °C cells is a result of faster kinetics, particularly for the sodium solid-state diffusion in the active materials. The poorer

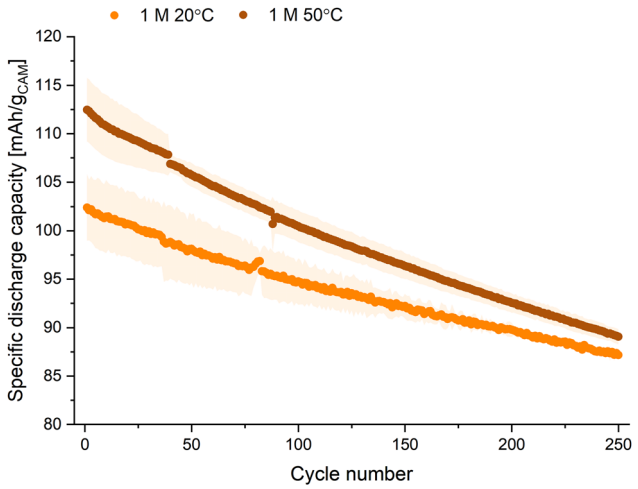

Fig. 4 Comparison of specific discharge capacity *vs.* cycle number at 20 °C and 50 °C for 1 M $NaPF_6$ in EC : DEC (1 : 1 v/v) electrolyte. The applied C-rate (C/2) was based on the expected capacity of 138 mA h g^{-1} of the NFM111 cathode, using cell voltage limits of 1.5 and 4.0 V. Error bars display standard deviation of 2-coin cells.

capacity retention is likely a result of accelerated electrolyte degradation and dissolution of thermally unstable components in the solid–electrolyte interphase (SEI).[27] This is not mitigated by using a higher Na^+ concentration electrolyte. The Coulombic efficiencies for the 1 M 20 °C and 50 °C cell cycling are similar throughout (Fig. S8 and S10, ESI†).

After 250 cycles, the capacities for both the 20 °C and 50 °C cells are approximately equal. When comparing the results of the lower electrolyte concentrations at either elevated temperature or room temperature to the 1 M $NaPF_6$ electrolyte, similar cycling performance was observed. Thus, the electrolytes with lower concentration performed comparably to the 1 M solution, both at 20 °C and 50 °C.

In conclusion, this work has investigated the effects of concentration of $NaPF_6$ electrolyte solutions. 1 M $NaPF_6$ in EC:DEC was found to give the highest bulk conductivity of the electrolytes studied. However, in sodium-ion coin cells using NFM111 and hard carbon electrodes, the lower concentration electrolytes gave comparable cycling performance to conventionally used 1 M $NaPF_6$ electrolyte. This was seen even at moderately high discharging rates of 2C. The main implication of this work is that reducing electrolyte concentration may be a route to reducing battery manufacturing costs while maintaining battery cycling performance.

DMCO, SO, TS, EK, DSW and CPG would like to thank The Faraday Institution for funding this work, FIRG064 and FIRG060. HES was supported by EPSRC award reference number EP/R513180/1.

Data availability

The data supporting this article have been included as part of the ESI.†

Conflicts of interest

There are no conflicts to declare.

Notes and references

1 T. Kim, W. Song, D.-Y. Son, L. K. Ono and Y. Qi, *J. Mater. Chem. A*, 2019, **7**, 2942–2964.
2 M. Armand, P. Axmann, D. Bresser, M. Copley, K. Edström, C. Ekberg, D. Guyomard, B. Lestriez, P. Novák, M. Petranikova, W. Porcher, S. Trabesinger, M. Wohlfahrt-Mehrens and H. Zhang, *J. Power Sources*, 2020, **479**, 228708.
3 Y. Miao, L. Liu, Y. Zhang, Q. Tan and J. Li, *J. Hazard. Mater.*, 2022, **425**, 127900.
4 M. Wentker, M. Greenwood, M. C. Asaba and J. Leker, *J. Energy Storage*, 2019, **26**, 101022.
5 M. Abdelbaky, J. R. Peeters, S. Van Den Eynde, I. Zaplana and W. Dewulf, *Procedia CIRP*, 2022, **105**, 7–12.
6 C. Vaalma, D. Buchholz, M. Weil and S. Passerini, *Nat. Rev. Mater.*, 2018, **3**, 18013.
7 J.-Y. Hwang, S.-T. Myung and Y.-K. Sun, *Chem. Soc. Rev.*, 2017, **46**, 3529–3614.
8 D. Alvira, D. Antorán and J. J. Manyà, *Chem. Eng. J.*, 2022, **447**, 137468.
9 H. Moon, A. Innocenti, H. Liu, H. Zhang, M. Weil, M. Zarrabeitia and S. Passerini, *ChemSusChem*, 2023, **16**, e202201713.
10 P. Zhu, D. Gastol, J. Marshall, R. Sommerville, V. Goodship and E. Kendrick, *J. Power Sources*, 2021, **485**, 229321.
11 A. Ponrouch, D. Monti, A. Boschin, B. Steen, P. Johansson and M. R. Palacín, *J. Mater. Chem. A*, 2015, **3**, 22–42.
12 H. Qu, W. Hu, Y. Huang, T. Zhang, H. Fang and F. Li, *Energy Fuels*, 2024, **38**, 12472–12486.
13 H. Chen, K. Chen, J. Yang, B. Liu, L. Luo, H. Li, L. Chen, A. Zhao, X. Liang, J. Feng, Y. Fang and Y. Cao, *J. Am. Chem. Soc.*, 2024, **146**, 15751–15760.
14 A. Ponrouch, E. Marchante, M. Courty, J.-M. Tarascon and M. R. Palacín, *Energy Environ. Sci.*, 2012, **5**, 8572–8583.
15 F. Cheng, M. Cao, Q. Li, C. Fang, J. Han and Y. Huang, *ACS Nano*, 2023, **17**, 18608–18615.
16 K. Xu, *Chem. Rev.*, 2014, **114**, 11503–11618.
17 G. G. Eshetu, S. Grugeon, H. Kim, S. Jeong, L. Wu, G. Gachot, S. Laruelle, M. Armand and S. Passerini, *ChemSusChem*, 2016, **9**, 462–471.
18 A. Konarov, H. J. Kim, H. Yashiro and S.-T. Myung, *J. Mater. Chem. A*, 2019, **7**, 13012–13018.
19 A. Bhide, J. Hofmann, A. Katharina Dürr, J. Janek and P. Adelhelm, *Phys. Chem. Chem. Phys.*, 2014, **16**, 1987–1998.
20 P. Barnes, K. Smith, R. Parrish, C. Jones, P. Skinner, E. Storch, Q. White, C. Deng, D. Karsann, M. L. Lau, J. J. Dumais, E. J. Dufek and H. Xiong, *J. Power Sources*, 2020, **447**, 227363.
21 C. Geng, D. Buchholz, G.-T. Kim, D. V. Carvalho, H. Zhang, L. G. Chagas and S. Passerini, *Small Methods*, 2019, **3**, 1800208.
22 D. Monti, E. Jónsson, A. Boschin, M. R. Palacín, A. Ponrouch and P. Johansson, *Phys. Chem. Chem. Phys.*, 2020, **22**, 22768–22777.
23 K. Chayambuka, R. Cardinaels, K. L. Gering, L. Raijmakers, G. Mulder, D. L. Danilov and P. H. L. Notten, *J. Power Sources*, 2021, **516**, 230658.
24 D. M. C. Ould, S. Menkin, C. A. O'Keefe, F. Coowar, J. Barker, C. P. Grey and D. S. Wright, *Angew. Chem., Int. Ed.*, 2021, **60**, 24882–24887.
25 J. Landesfeind, T. Hosaka, M. Graf, K. Kubota, S. Komaba and H. A. Gasteiger, *J. Electrochem. Soc.*, 2021, **168**, 040538.
26 G. A. Giffin, *Nat. Commun.*, 2022, **13**, 5250.
27 E. Peled and S. Menkin, *J. Electrochem. Soc.*, 2017, **164**, A1703–A1719.